NOTICE CONCERNING COPYRIGHT RESTRICTIONS

A Depletion Mechanism for the Behavior of Noncondensible Gases at The Geysers

Tom Powell[1] and Kewen Li[2]

[1]Thermochem Inc., Santa Rosa, CA
[2]Stanford University, Stanford, CA

Keywords

The Geysers, noncondensible gases, porosity, capillary pressure, vapor-dominated systems

ABSTRACT

Vapor-dominated geothermal systems, including The Geysers and Larderello, have experienced significant increases in noncondensible gas during their productive histories. A depletion model has been developed to explain these increases. In the model, the low permeability of the reservoir rock matrix initially retards the flow of vapor through the matrix to fractures due to the plugging effect of capillary water. Steam produced early in the life of the field is predominantly from evaporated pore water near fractures and has a low gas concentration. Declining pore pressure in the rock matrix induces boiling of reservoir liquid, resulting in the formation of gas-rich vapor bubbles in larger pores. Gas concentrations of produced steam increase when vaporization of the capillary water in the fine permeable channels of the rock matrix opens pathways for the trapped gas-rich vapor to escape to the reservoir fracture network. Calculations show that steam-water capillary pressures of the matrix at reservoir conditions were great enough to block the flow of the vapor.

The Geysers fluids can be modeled as a mixture of vaporized reservoir liquid and gas-rich vapor, in a manner similar to the Y model used in gas geothermometry. Gas dissolved in initial reservoir liquid is derived largely from organic material in the greywacke reservoir rock and reactions with reservoir minerals. Although important reservoir parameters, such as steam-water relative permeability, need to be determined at reservoir conditions, this model holds promise that the noncondensible gas evolution of The Geysers, Larderello and other vapor fields might be quantified and predicted.

Introduction

Noncondensible gas concentrations in geothermal fields often show disconcerting increases as fields mature. The gas increases
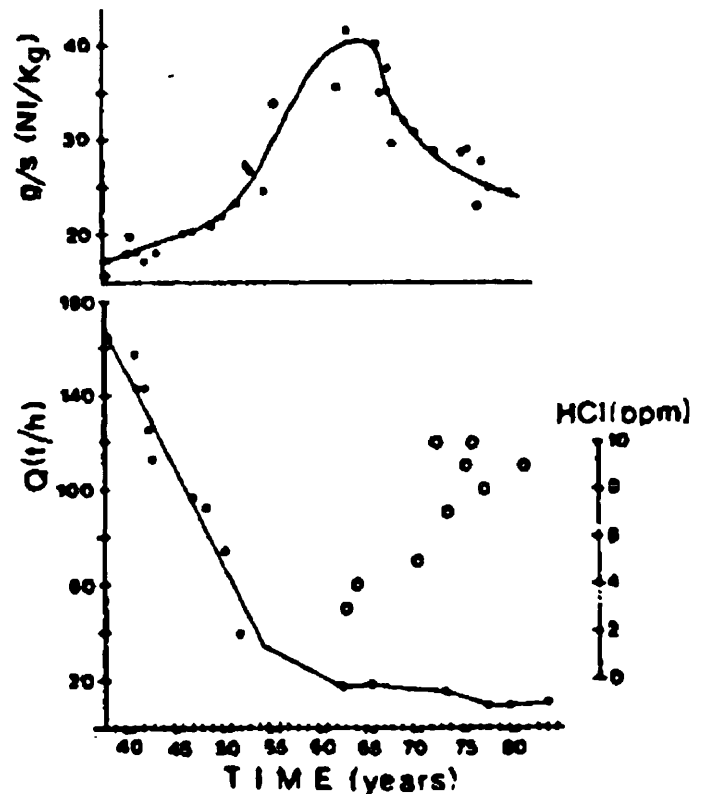
Figure 1. Flow rate and gas/steam ratio of steam from Larderello well ALR (from D'Amore & Pruess, 1985).

have been observed both at Larderello, Italy and at The Geysers, California. Figure 1 shows the history of gas change for Larderello well ALR. Note that the gas/steam ratio in the well was low during initial production, then rose as the steam flow rate declined. The gas/steam ratio peaked at approximately four times the initial concentration at about the time that the steam flow rate decline stabilized at a low rate and the volatile chloride (here measured as HCl in steam condensate) first appeared in steam. The appearance of volatile chloride in steam has been interpreted to indicate severe dry-out of the steam reservoir (Truesdell *et al.*, 1989).

These gas increases are not welcome developments. Minor increases above power plant design specifications reduce plant efficiency and increase steam usage. Further increases require retrofit of condenser gas extraction and gas abatement equipment.

Gas increases also present a problem for geothermal projects in the emerging greenhouse gas credit market. How does a geothermal developer sell credits for a project when the long-term gas emissions can not be reliably predicted?

To date, there has been little scientific consensus on the source of gas in the reservoir and the cause of gas increases. The most commonly held assumption is that gases are stored with water reserves in pore spaces of the reservoir rock, and are produced with the steam as the reservoir is depleted. For example, D'Amore and Truesdell (1985) assumed this process in calculating reservoir liquid saturation using gas geothermometry. Gas increases in the central, low-pressure production areas of the field are attributed to steam migration from gassy field margins (e.g. Truesdell *et al.*, 1993).

On the other hand, Beall and Box (1993) showed that gas concentrations in the SE Geysers followed an inverse relationship with steam flow rate. They suggested that this might be due to migration of gas from regional sources because of decreasing reservoir pressure.

Pruess *et al.* (1985) showed that CO_2 gas concentrations from Larderello wells exceeded the amount that could be stored in two-phase fluid in the reservoir matrix, and additional gas was supplied either from an external source, or (more likely) due to the breakdown of carbonate minerals.

A common aspect of all these models is that, prior to extensive production, they offer little basis for the prediction of gas behavior during production. Lacking an empirical gas–flowrate correlation, like that found for the SE Geysers by Beall and Box (1993), field operators have no way to predict future gas changes, nor the greenhouse emissions from a field. Models evoking mineral reactions or the influx of gas either from field margins or regional sources would be unconstrained. If gas behavior is ever to be predicted, it will require a model based upon what can be known about a reservoir, in an approach similar to modern-day reservoir simulation.

This study presents a model for the gas increases observed at The Geysers based upon in-place gas depletion from the reservoir. In creating this model, we draw upon gas geochemistry studies to explain the initial gas concentrations in the reservoir matrix, and then show how the properties of the reservoir rock matrix act to control the behavior of gas in produced steam.

Gas Behavoir at The Geysers

Gas behavior at The Geysers has followed a similar, although locally more dramatic, path to that previously presented for Larderello. Figure 2 shows the evolution of gas concentration and chemistry in well GDCF 63A-29. The gas concentration of the well increased by more than a factor of 5 over a period of 4 years, and was subsequently arrested and reversed by water injection. The mole fractions of the two relatively soluble gases, H_2S and NH_3, both decreased as gas concentration increased. Following injection, the mole fractions of these two gases increased again, largely due to their presence in injectate.
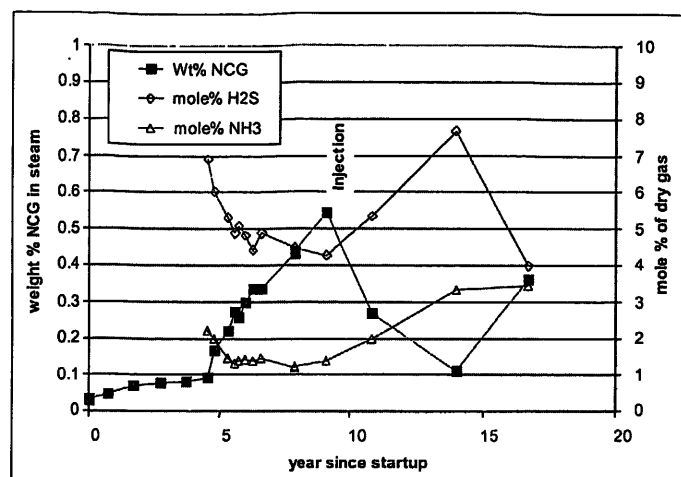

Figure 2. Total noncondensible gas and mole fraction H_2S and NH_3 changes for well GDCF 63A-29 in the central Geysers.
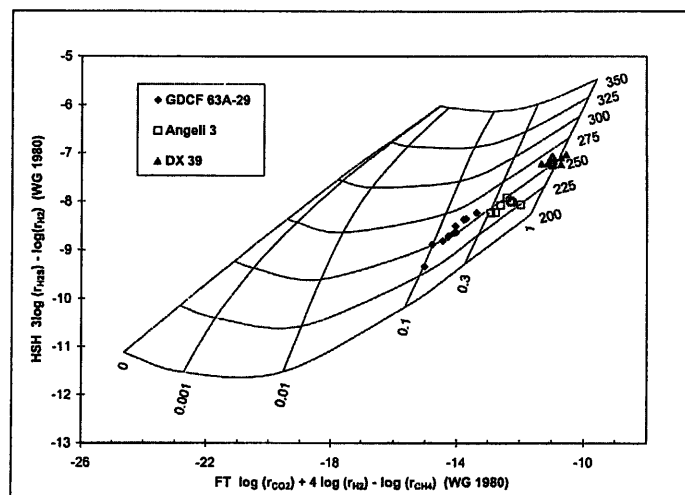

Figure 3. Gas geothermometer grid plot of the Fischer-Tropsch (methane breakdown) and hydrogen-hydrogen sulfide (HSH) reactions. Gas compositions are for wells that show gas increases independent of injection processes. Gas increases proceed from the left to right.

The implication of this is that gas fractionation between liquid and vapor plays a role in the behavior of noncondensible gas at The Geysers. As zones of reservoir are depleted, gas concentrations increase and the proportions of the more soluble gases (H_2S and NH_3) decrease.

Another clue to the behavior of gas at The Geysers is the success of the Y model in gas geothermometry (e.g. D'Amore and Truesdell, 1985). The Y model addresses the ambiguity in gas geothermometry introduced by the inherent differences in gas concentrations and proportions of gases in liquid water in the reservoir as compared to those in coexisting steam. Water in equilbrium with reservoir gases and minerals will have a much lower gas concentration and different mix of gases than steam under the same pressure-temperature conditions. The Y model assumes that water and steam in the reservoir are in equilibrium with each other and with the chemical reactions underlying the geothermometers, and that produced steam is a simple mixture of this reservoir steam and vaporized reservoir water.
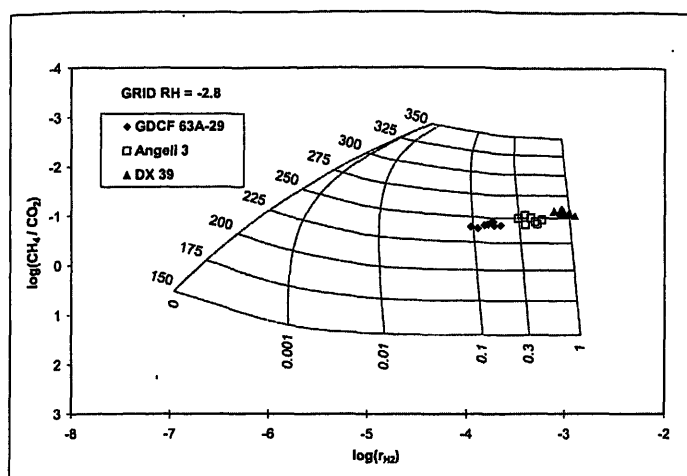
Figure 4. H$_2$-CH$_4$/CO$_2$ geothermometer grid set at RH –2.8.

Reservoir temperatures at The Geysers are consistent with selected geothermometer reactions. Figure 4 shows a plot of the noncondensible gases in steam from 3 widely separated Geysers wells on a geothermometer grid, similar to those proposed by Giggenbach (1980). Geothermometer temperatures for the 3 wells are close to the measured reservoir temperature (240-260°C). Trends of increasing Y follow with increasing gas concentration in these wells.

The success of this model in predicting reservoir temperature suggests that the process by which steam is produced from the reservoir rock involves segregation and mixing of a low-gas vaporized liquid and a high-gas reservoir steam. The success of gas geothermometry further suggests that gas concentrations in the reservoir are controlled by geochemical reactions, and therefore, initial gas concentrations might be calculated based upon temperature and chemical equilibria.

Core Properties

Important clues as to the process in the reservoir rock that might produce this gas behavior come from studies of the electrical resistivity of Geysers core samples under production conditions, and studies of the porosity and permeability in the core. A series of experiments testing the electrical resistivity of The Geysers core from Scientific Corehole Sulfur Bank 15D show that boiling and vapor formation in core samples occurs gradually as pressure decreases, rather than abruptly at the boiling conditions of freestanding water (Roberts et. al., 2001). Vapor replacement of liquid water in the core was inferred by an increase in electrical resistivity observed at pressure-temperature conditions above the boiling point. The authors attributed gradual vapor formation to the effect of capillary pressure in the pore spaces of the rock, in a model termed "inhomogeneous boiling". Vapor would form only in pore spaces where the capillary pressure was less than or equal to the vapor pressure (of the freestanding pore fluid) minus the pore pressure. As pore pressure was decreased (at constant temperature) vapor first formed in relatively large pore spaces where capillary pressure was low, and then progressed to finer and finer pores.

Based upon the pore size distribution of the core samples and the inhomogeneous boiling model, Roberts et al. (2001) showed

that 8-10% of pore space in the sample (at 145°C) became vapor-filled when pore pressure had been lowered to the point where the core temperature was 40-45°C above boiling. They suggested that boiling and vapor filling might happen in pores greater than ~0.4 μm in diameter.

Roberts et al. (2001) also observed negligible flow of liquid through the core, even with as much as 1.6 MPa pressure drop across the 1.5 cm-long core sample. This is consistent with very low matrix permeability. Persoff and Hulen (1996) measured matrix permeabilities ranging from 1.3 to 26 nanodarcies on SB-15D core samples from above and within the reservoir. Williamson (1980) reported permeability measurements of 0.1-0.5 microdarcy on 1-inch Geysers core samples, but stated that measurements on larger (4-inch) cores were dominated by microfractures and yielded greater values.

Petrographic analysis of The Geysers cores reported by Gunderson (1990) shows that most of the porosity visible at microscopic scale exists as vugs and voids in sealed veins, vein selvages and the rock matrix, and as fractures. This observation, along with that of very low matrix permeability, paints a very different picture of The Geysers reservoir rock than the rock with high permeability in petroleum reservoirs. The matrix of The Geysers reservoir rock appears to be characterized by dispersed pores surrounded by relatively tight rock matrix, crosscut by permeable fractures. This description of the reservoir rock matrix is the starting point for the model of noncondensible gas behavior during reservoir exploitation.

Gas Chemistry

Where is the gas stored in the reservoir? Noncondensible gas in the pre-production Geysers reservoir can reside in one of two phases, either dissolved in the liquid phase in the reservoir rock pores or mixed with the vapor phase in the fracture network and large pores. Vapor circulation characterizes the chemistry and thermodynamics of vapor dominated systems and the fracture network is its likely domain. Only large pores would be capable of hosting reservoir vapor because capillary pressure would cause pores below a certain size to be liquid-filled. Numerical simulation modeling of The Geysers field suggested that the initial liquid saturation of the rock matrix was around 80% (Williamson, 1992), implying that the other 20% was initially vapor filled.

Under equilibrium conditions the gas concentrations in these two phases would be determined by Henry's law gas partitioning between the liquid and vapor phases. The conformity of Geysers gases to certain geothermometer reactions allows reservoir gas concentrations to be calculated. For well GDCF 63A-29, featured in Figures 2 and 3, the concentration of gas in reservoir liquid is modeled to be 0.012 wt% and that in an equilibrium vapor phase 1.4 wt%. It is clear from Figure 2, and from early gas concentrations measured throughout the field, that the first production from the reservoir was closer in gas concentration to that of a vaporized liquid phase than that equilibrium vapor. This is difficult to reconcile with the notion that the earliest production from the field would have been mostly steam from the fracture network, and under equilibrium conditions this steam should have had a gas concentration closer to that of the equilibrium vapor.

Gunderson (1989) provided an answer to this problem. Based upon the similarity in the aerial distribution of gas concentration and the distribution and depth of felsite, he proposed that reservoir gas originates in the reservoir rock migrates to the fracture network and is swept to the top of the reservoir or to surface discharge. High gas appears in areas with a thick greywacke section above felsite, and low gas appears where the greywacke reservoir is thin and felsite is shallow.

Given a steady supply of gases from the breakdown of organic material in the sedimentary greywacke reservoir rock, geochemical reactions can account for nearly all of the gases observed in the steam, as the success of the two gas geothermometers in Figure 4 demonstrates. Organic methane breaks down to form carbon dioxide and hydrogen; hydrogen reacts with pyrite to form hydrogen sulfide and magnetite. An organic source for the CO_2 at The Geysers is consistent with the carbon isotopes (Huebner, 1981). Organic nitrogen and ammonia do not attain equilibrium due to the very high temperature requirements of the ammonia breakdown reaction (Giggenbach, 1987), and this is confirmed by the general failure of this geothermometer at The Geysers. Ammonia appears to be favored in the formation of the organic nitrogen gases creating an excess of ammonia in the reservoir gases, as noted by Lowenstern, *et al.* (1999). Nitrogen and argon are probably introduced by circulation of meteoric groundwater into the reservoir, as suggested by the meteoric water component observed in the stable isotopes of steam (Gunderson, 1989). Some argon may also originate from potassium-40 decay. Kennedy and Truesdell (1994) reported a good case for an igneous source of much of the gas in the NW Geysers, so there likely is a component of magmatic gas in the reservoir, as well.

The limit on these reactions is expected to be hydrogen concentration, which is controlled by the temperature and redox dependent hydrolysis reaction of water to form hydrogen and molecular oxygen. At some point an oversupply of hydrogen would trigger conversion to H_2O, forcing the system to a more reducing chemical environment. Redox in the reservoir appears to be controlled by the Fe^{+2}/Fe^{+3} buffer at R_H -2.8, however, consistent with that found by Giggenbach (1987) for most mature volcanic-hosted geothermal systems. R_H is the log ratio of hydrogen fugacity to water vapor fugacity, and is a convenient measure of chemical oxidation-reduction potential in geothermal systems. Gas data from the three wells are plotted on an R_H-dependent geothermometer grid in Figure 4. This grid plots the hydrogen geothermometer versus log (CH_4/CO_2), based upon the methane breakdown reaction, at R_H -2.8. The gas data plot at essentially the same positions they do for the R_H-independent geothermometers in Figure 3, suggesting that system redox potential is controlled by the iron buffer. Upon more detailed modeling, it has been found that data from the highest gas well, DX-39, best matches with slightly higher temperature (280°C) and slightly more reducing R_H (-2.72), suggesting that hydrogen production probably outpaces the iron buffer in high-gas areas of the reservoir.

Gas Behavior Model

The model proposed for the gas behavior in The Geysers reservoir includes aspects of both the porosity/permeability characteristics of the reservoir rock matrix, and the chemistry of
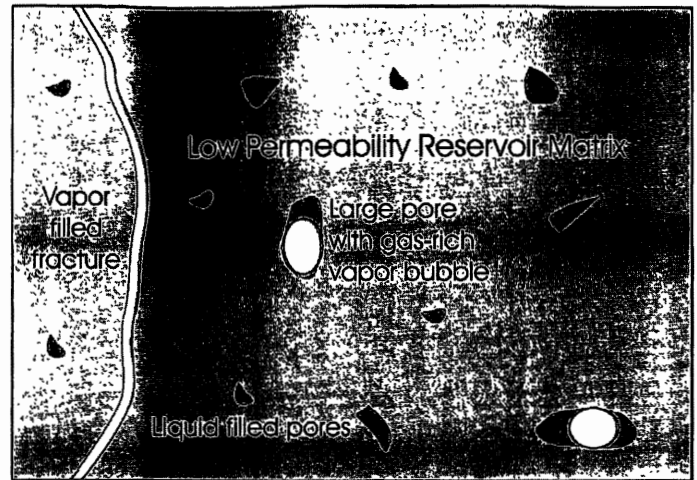

Figure 5. Diagrammatic representation of reservoir matrix.

the gases. The pre-production reservoir matrix, as envisioned in Figure 5, consists of low-permeability metamorphosed sandstone (greywacke) pitted with pores and voids. Initial liquid water saturation in the matrix is around 80%, as suggested by numerical simulation (Williamson, 1992) and laboratory studies (Li and Horne, 2003). The liquid phase contains equilibrium concentrations of most of the major noncondensible gases. Some larger pores are vapor filled (grey bubbles), with gas concentration in Henry's law equilibrium with the gas dissolved in the liquid phase. In the case of GDCF 63A-29, this vapor would have a total gas concentration of approximately 1.4 wt%, over two orders of magnitude higher than the gas concentration in the liquid phase (0.012 wt%). Under initial steady state conditions, gas probably diffused through the matrix to the fractures and was swept away by steam convection.

At the onset of production, the vapor pressure in the fracture drops and liquid in and around the fracture begins to vaporize and flow through the fracture network to the well. Early steam is low in gas concentration because it is essentially boiled liquid from the near-fracture environment. The pressure gradient established between fracture and matrix causes liquid and vapor in the matrix to migrate toward the fracture, but due to the small permeable channels in the matrix most channels are filled with capillary water. Liquid vaporizes at the steam-water interface in accordance with the lowered vapor pressure at the capillary interface. The end result is that only very little of the vapor trapped in pores is allowed to escape to the fracture. Liquid held in the fine permeable channels of the matrix blocks its release.

Decreased pore pressure in the near-fracture matrix causes another process to begin in the pore space. As the difference between pore pressure and vapor pressure increases, vapor bubbles now form in some of the smaller pores and existing bubbles grow to accommodate greater capillary interface curvatures. Dissolved gas in matrix liquid now has a local vapor phase into which it can partition, depleting the gas in the matrix liquid phase and retaining gas in the matrix vapor. This process is depicted diagrammatically in Figures 6 and 7.

Figure 8 shows the conditions in the reservoir matrix after prolonged production. Pore pressure in the rock decreases, permeable channels in the matrix dry out and high-gas vapor trapped
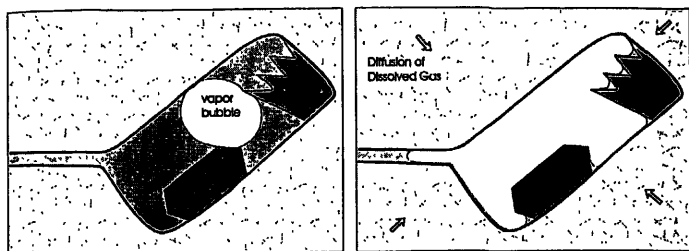
Figure 6. Existing vapor bubble in matrix pore grows with decreased pore pressure, scavenging gas from surrounding matrix liquid. The vapor bubble in the pore is blocked from escaping by capillary liquid in the channel connecting it with the fracture network.
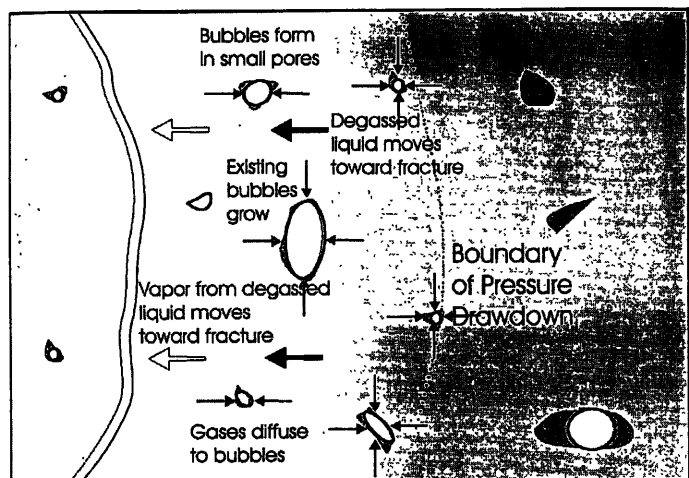

Figure 7. Matrix liquid migrates toward fracture and vaporizes. Vapor bubbles grow in pore spaces, scavenging gases from liquid.
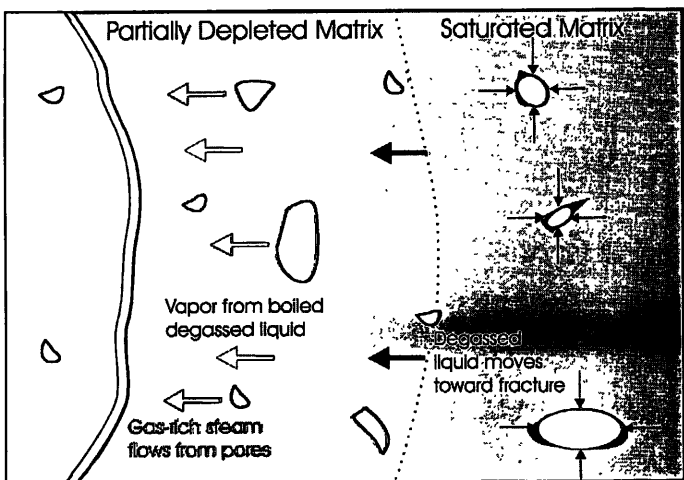

Figure 8. Rock matrix near fracture dries out, releasing high-gas vapor trapped in pores.

in pores is released. Gas concentrations in produced steam rise in response.

Ultimately, the rock matrix dries out to the point where no vapor-filled pores are isolated, and only liquid water held in the smallest pore throats is available for vaporization. There is no more gas stored in pores and gas concentrations at the wellhead decline.

As a first approximation steam produced from this matrix rock is a mixture of vaporized reservoir liquid, from evaporating capillary water, and reservoir vapor from vapor bubbles in pores. Figure 9 shows the comparison of the gas data from well GDCF 63A-29 with Y model trends for reservoir fluid. The plot shows gas/CO_2 ratios for different gases, plotted versus CO_2 concentration. Thus, relative changes in gas concentration of constituent gases can be observed along with changes in the gas concentration of the principal gas, CO_2. The Y model trends, which would appear as straight mixing lines in linear-linear plot space, appear curved in log-log space. Gas concentrations for the trends of hydrogen, hydrogen sulfide and methane are constrained by geothermometer reactions.

It can be seen in Figure 9 that the Y model makes a reasonably good fit with the data for the different gases, although data trends for H_2, H_2S and CH_4 do not match the mixing trends of the Y model. The mismatch in trends appears to be because of a
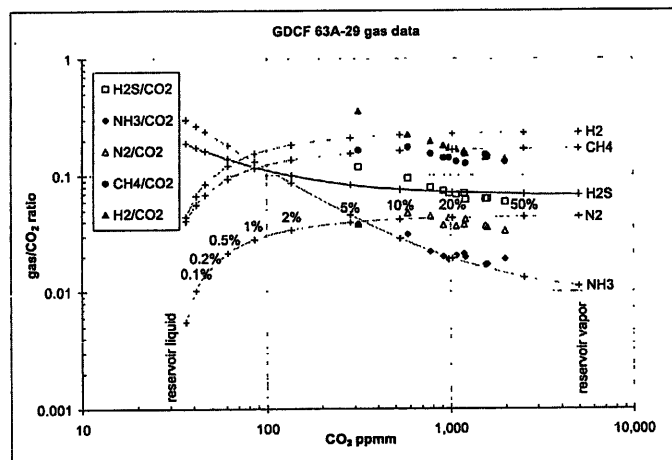

Figure 9. GDCF 63A-29 gas data plotted as ratios to CO_2, versus CO_2 concentration in ppm molar in log-log space. Starting point of trends on left are reservoir liquid concentration based upon geothermometer reactions.
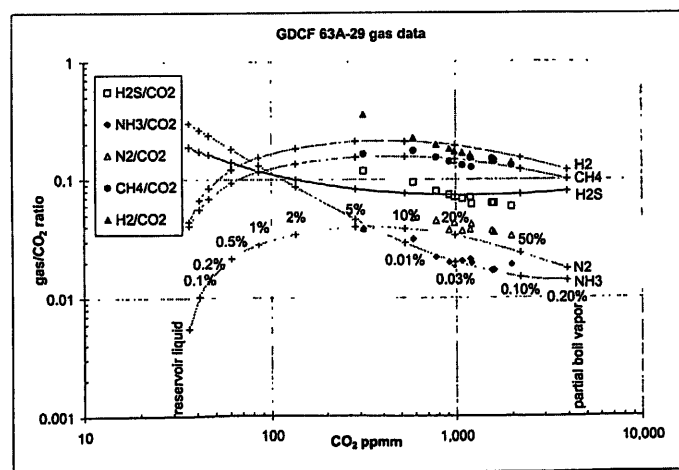

Figure 10. GDCF 63A-29 gas data matched to modified Y model trends. Percentages along the ammonia trend show the fraction of the vapor endmember in a partial boil (e.g. for 0.03% the vapor fraction represents 0.03% steam separation).

change in the vapor endmember gas composition with time. The model predicts that the early vapor endmember would be essentially in Henrys law equilibrium with reservoir liquid, whereas later vapor would be from expanded vapor bubbles, enriched by gas scavenged from reservoir liquid. The factor limiting the gas concentration of the later vapor is the amount of gas available from the reservoir liquid, the less soluble gases being more limited in supply than the more soluble gases.

Figure 10 shows the mixing trends expected if the high-gas endmember represents an increasing partial boil fraction of reservoir liquid. In other words, as the fraction of equilibrated reservoir vapor increases, it increasingly represents a partial boil of reservoir liquid. This is what would be expected with vapor bubble growth and new vapor bubble formation as pore pressure in the rock matrix decreases.

The partial boil model in Figure 10 does a better job of matching all the gas data except H_2S, whose data also showed a relatively poor match with the Y model trend. It is not clear why H_2S is anomalous, although a close correspondence between H_2S and H_2 at The Geysers has been previously noted by Lowenstern et al. (1999). Hydrogen may exert close geochemical control over H_2S concentration, masking the effects of pure Henry's law solubility processes.

Discussion

The inhibition of vapor movement in the rock matrix seemingly violates the usual notion of relative permeability in a vapor-dominated geothermal system. If water saturation in the system is initially at the irreducible minimum, as expected in a vapor-dominated system, then the vapor should be mobile at initial conditions. In the usual Corey-type relative permeability relationship, if one phase is immobile, the other is mobile.

This must certainly be true in the fracture network of the system since vapor is the circulating fluid of the system. The high capillary pressure of the matrix, however, acts both to maintain a high liquid water saturation, and inhibit the flow of vapor. To demonstrate the possibility of the inhibition of vapor movement by capillary pressure in the matrix, firstly it is necessary to estimate the value of the steam-water capillary pressure of the matrix at The Geysers reservoir conditions. This is discussed as follows.

Experimental data of steam-water capillary pressure of The Geysers rock at reservoir conditions are not available in the literature. However, Li and Horne (2002) developed a steam-water capillary pressure model based on the measurements of steam-water capillary pressure in Berea sandstone at about 120°C (Li and Horne, 2001) and the vapor-water capillary pressure data in The Geysers rock at room temperature measured (Persoff and Hulen, 1996). According to this model, steam-water capillary pressure can be calculated once porosity, permeability, reservoir temperature are known. The model is expressed as follows:

$$P_c = 4.012 \frac{\sigma}{\sqrt{\frac{k}{\phi}}} (S_{wd}^*)^{-1.843}$$

(1)

where S_{wd}^* are the normalized water saturation, P_c is the capillary pressure, k and ϕ are permeability and porosity, σ is the surface

tension. The units of P_c, σ and k are MPa, dynes/cm, and nd respectively; ϕ and S_{wd}^* are expressed as fractions. The porosity and permeability of reservoir rocks can be measured. The surface tension can be calculated once the reservoir temperature is known. The model expressed in Eq. 1 is suitable for drainage process and is based on the assumptions: (1) contact angle does not change with permeability and temperature; (2) rock samples have the same J-functions.

According to the experimental data reported by Persoff and Hulen (1996), we chose a porosity of 1.9% for The Geysers reservoir rock. This value is also in the range from 1.2 to 4.6% reported by Williamson (1991). Similarly we chose a permeability of 1.3 nd as the lower limit for the matrix of The Geysers reservoir rock and a permeability of 500 nd as the upper limit. The surface tension at 240°C, chosen as the reservoir temperature, is 28.41 mN/m (Yaws, 1999). Steam-water capillary pressure at reservoir conditions were then calculated using these values according to Eq. 1 and the results are shown in Figure 11. One can see from Figure 11 that the steam-water capillary pressure of the rock matrix at reservoir conditions is huge and is great enough to block the
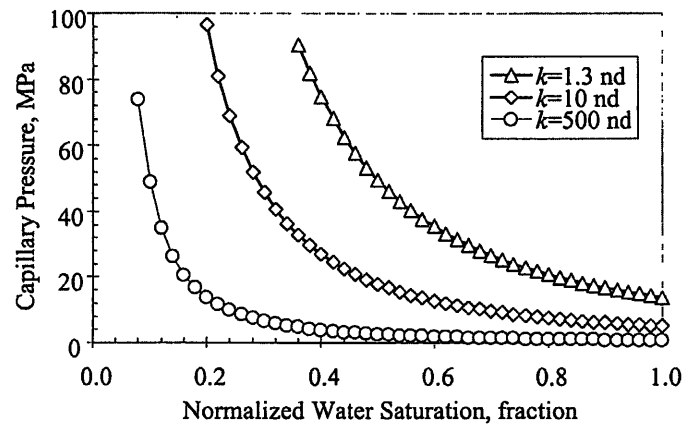

Figure 11. Steam-water capillary pressure curves at a temperature of 240°C for rock with different permeability. Initial reservoir pressure at The Geysers was approximately 3.5 MPa.
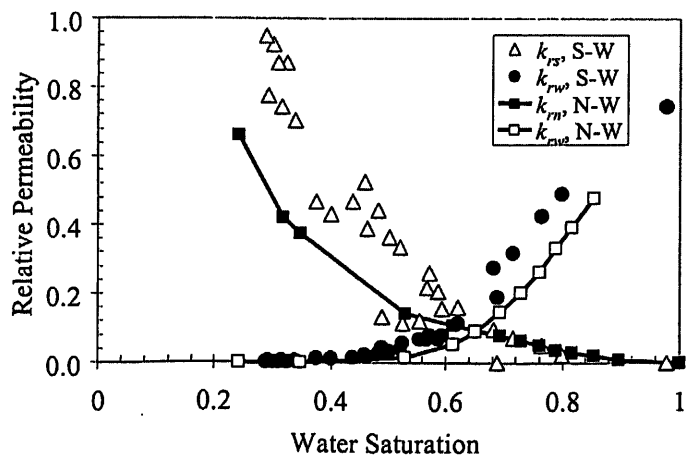

Figure 12. Steam-water (S-W) and nitrogen-water (N-W) relative permeability curves at a temperature of 120°C in Berea sandstone.

flow of vapor in the matrix, even for the matrix with permeability at upper limit.

If the water in the matrix seriously inhibits the flow of vapor, the vapor (steam) relative permeability must be very low. Steam-water relative permeability relationships for The Geysers at reservoir conditions have yet to be determined, but steam-water relative permeability data measured on Berea sandstone at about 120°C were reported by Horne et al. (2000). The relative permeability data of both steam-water and nitrogen-water flow are plotted in Figure 12. One can see that vapor remains immobile until roughly 80% liquid saturation. This is close to the 70-80% initial liquid saturation at The Geysers geothermal field, as cited previously. The observation suggests the strong possibility that vapor in the rock matrix may not be mobile at initial conditions.

On the other hand, the vapor (steam) relative permeability in the matrix may be extremely low even if the vapor phase is mobile. As Li and Horne (2003) reported, the irreducible water saturation measured at about 120°C in a core sample from The Geysers geothermal field was about 70%. According to Figure 12, the vapor relative permeability in the matrix is very low at this water saturation even in Berea sandstone.

Note that some of the discussion in this section was based on the experimental data measured in Berea sandstone. It is necessary to verify the discussion by additional core tests in The Geysers rock under reservoir conditions. Stanford Geothermal Program has embarked on a research on this subject.

Conclusions

The model presented here shows that the gas increases observed at The Geysers, and potentially other vapor-dominated geothermal fields can be explained by an integration of gas chemistry with the porosity structure and production characteristics of Geysers reservoir rock. With this comes the possibility that gas behavior, and the amount of stored gas in a geothermal reservoir, might be predicted based upon gas geothermometry and reservoir rock properties.

This would not be without challenges and the need for further research, however. There is incomplete understanding of relative permeability and liquid saturation at reservoir conditions. The analysis presented here shows that this process for gas storage and release from the rock matrix is plausible, but quantification of these properties will be required for a rigorous prediction.

A calculation of the gas produced at The Geysers versus that calculated to be stored in the reservoir would provide a test of this hypothesis. This will be attempted in a follow-up paper.

Besides vapor systems, this model may have application to liquid dominated geothermal systems, where gas increases have also been observed. Provided similar matrix permeability and pore size distribution, gas rich vapor would be expected to accumulate in pores in a similar fashion to vapor systems. Stimac et al. (2003) report similar porosity and permeability in the Mat-25 core, Tiwi Field, Philippines, to that found by Gunderson (1990) in The Geysers. The large pores in the Mat-25 core are due to mineral grain dissolution and replacement, which is likely a common pore-forming process in hydrothermally altered reservoir rocks.

Acknowledgements

References

Beall, J.J. and Box, W.T., 1993, The future of noncondensible gas in the Southeast Geysers Steamfield; GRC Trans. Vol. 17, pp. 221-225.D'Amore, F. and Truesdell, A.H., 1979, Models for steam chemistry at Larderello and The Geysers, Proc. 4th Workshop on Reservoir Engineering, Stanford University, California, pp. 262-276.

D'Amore, F. and Pruess, K., 1985, Correlation between vapor saturation, fluid composition and well decline in Larderello; Proc. 10th Workshop on Reservoir Engineering, Stanford University, California, Jan. 22-24, 1985, pp. 113-121.

D'Amore, F. and Truesdell, A.H., 1985, Calculation of geothermal reservoir temperatures and steam fraction from gas compositions; GRC Trans., Vol. 9-1, pp. 305-310.

Giggenbach, W.F., 1980, Geothermal gas equilibria; Geochimica et Cosmochimica Acta, Vol. 44, pp. 2021-2032

Giggenbach, W.F, 1987, Redox processes governing the chemistry of fumarolic discharges from White Island, New Zealand; Applied Geochemistry, Vol. 2, pp. 143-161.

Gunderson, R.P., 1989, Distribution of oxygen isotopes and non-condensable gas in steam at The Geysers; GRC Trans. Vol. 13, pp. 449-454.

Gunderson, R.P., 1990, Reservoir matrix porosity at the Geysers from core measurements; GRC Trans Vol. 14, pp. 1661-1665.

Horne, R.N., Satik, C., Mahiya, G., Li, K., Ambusso, W., Tovar, R., Wang, C., and Nassori, H., 2000, Steam-Water Relative Permeability, presented at World Geothermal Congress, Kyushu-Tohoku, Japan, May 28-June 10, 2000; GRC Trans. V. 24 (2000).

Huebner, M., 1981, Carbon-13 isotope values for carbon dioxide gas and dissolved carbon species in springs and wells in The Geysers-Clear Lake region; in USGS Prof. Paper 1141, pp. 211-213.

Kennedy, B.M., and Truesdell, A.H., 1994, Active magmatic degassing in the NW Geysers high-temperature reservoir; GRC Trans., Vol. 18, pp. 325-330.

Li, K. and Horne, R.N., 2002, A Capillary Pressure Model for Geothermal Reservoirs, Proceedings of the GRC 2002 annual meeting, September 23-25, 2002, Reno, USA; GRC Trans. V. 26 (2002).

Li, K. and Horne, R.N., 2001, An Experimental and Theoretical Study of Steam-Water Capillary Pressure, SPEREE (December 2001), p.477-482.

Li, K. and Horne, R.N., 2003, Direct measurement of in-situ water saturation in The Geysers rock, Proc. 28th Workshop on Reservoir Engineering, Stanford University, California, Jan 27-29, 2003.

Lowenstern, J.B., Janik, C.J., Fahlquist, L.S. and Johnson, L.S., 1999, Gas and isotope geochemistry of 81 steam samples from wells in The Geysers geothermal field, Sonoma and Lake counties, California, U.S.A.; USGS Open-File Report 99-304.

Persoff, P. and Hulen, J.B, 1996, Hydrologic characterization of four cores from The Geysers Coring Project; Proc. 21st Workshop on Reservoir Engineering, Stanford University, California, Jan 22-24, 1996, pp. 327-334.

Pruess, K., Celati, R., Calore, C. and D'Amore, F., 1985, CO2 trends in the depletion of the Larderello vapor-dominated reservoir; Proc. 10th Workshop on Reservoir Engineering, Stanford University, California, Jan. 22-24, 1985, pp. 273-278.

Roberts, J.J., Duba, A.G. Bonner, B.P. and Kasameyer, P.W., 2001, *The effects of capillarity on electrical resistivity during boiling in metashale from Scientific Corehole SB-15-D, The Geysers, California, USA*; Geothermics Vol. 30, No. 2-3, pp. 235-254.

Satik, C., Walters, M. and Horne, R.N., 1996, *Adsorption characteristics of rocks from vapor-dominated geothermal reservoirs at The Geysers, CA*; Proc. 21th Workshop on Reservoir Engineering, Stanford University, California, Jan. 22-24, 1996, pp. 469-480.

Stimac, J.A., Powell, T.S., Golla, G.U., 2003, *Porosity and permeability of the Tiwi geothermal field, Philippines based on continuous and spot core measurement;* Geothermics, in press.

Truesdell, A., Enedy, S., and Smith, B., 1993, *Geochemical studies of reservoir processes in the NCPA field of The Geysers a Preliminary Report*; Proc. 18th Workshop on Reservoir Engineering, Stanford University, California, pp. 35-43

Truesdell, A.H., Haizlip, J.R., Armannsson, H. and D'Amore, F., 1989, *Origin and transport of chloride in superheated geothermal steam*; Geothermics, Vol. 18, No. 1/2, pp. 295-304.

Yaws, C.L., 1999, *Chemical Properties Handbook*; Mcgraw-Hill.

Williamson, K.H., 1992, *Development of a reservoir model for The Geysers geothermal field*, GRC Special Report #17 (Monograph on the Geysers Geothermal Field), pp. 179-197.